ACS Catalysis

Letter

pubs.acs.org/acscatalysis

Novel Hierarchical Cerium-Incorporated MFI Zeolite Catalysts for the Catalytic Fast Pyrolysis of Lignocellulosic Biomass

Gregory T. Neumann and Jason C. Hicks*

Department of Chemical and Biomolecular Engineering, University of Notre Dame, 182 Fitzpatrick Hall, Notre Dame, Indiana 46556, United States

Supporting Information

ABSTRACT: We report the synthesis of a new multifunctional mesoporous zeolite catalyst with cerium incorporated within the framework. This catalyst shows a shift in selectivity from typical HZSM-5 products (benzene, toluene, and xylenes) to valuable oxygenated chemicals (furans, ketones, aldehydes) during the catalytic fast pyrolysis of lignocellulosic biomass. The cerium-incorporated hierarchical zeolite was synthesized using a dry-gel method followed by steam-assisted crystallization. The catalyst was characterized by X-ray diffraction (XRD), N_2 physisorption, scanning electron microscopy (SEM), scanning transmission electron microscopy (STEM), transmission electron microscopy (TEM), NH_3 temperature-programmed desorption (NH_3-TPD), diffuse reflectance FT-IR, and diffuse reflectance UV−Visible (UV−Vis) spectroscopy. The multifunctional catalyst was then studied in the catalytic fast pyrolysis of glucose (a carbohydrate model compound) at 600 °C. The new catalyst was compared with a mesoporous HZSM-5 catalyst with incipient wetness incorporated cerium and an ion exchanged commercial HZSM-5 catalyst. These catalysts behaved similarly to the parent materials, but the new catalyst with cerium incorporated into the zeolite framework exhibited selectivities greatly shifted from aromatics to oxygenated chemicals. Furthermore, this catalyst produced less coke (40 wt % or 11 mol % carbon) and increased CO production through decarbonylation reactions. These properties persisted after catalyst regeneration and recycle.

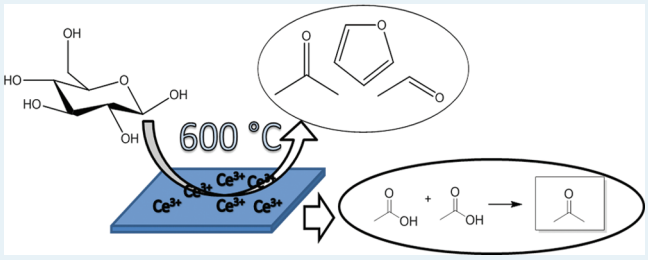

KEYWORDS: *ZSM-5, hierarchical, biofuels, mesoporous, zeolite, lignocellulosic, biomass, fast pyrolysis, cerium*

Petroleum-based resources are currently society's primary source of chemicals and transportation fuels. However, because of factors such as the finite reserves of petroleum, their unequal geographic distributions, and the environmentally motivated desire to decrease CO_2 emissions, renewable energy sources, such as lignocellulosic biomass, have become promising candidates for the production of renewable fuels and chemicals.[1−3] To effectively use these abundant resources, particularly with existing infrastructure, these highly oxygenated feedstocks must be chemically converted into products that are more stable and more similar to currently used fuels and chemicals. Thermochemical methods, such as catalytic fast pyrolysis, have been widely studied as potentially scalable processes to convert solid biomass feedstocks into high energy density liquids or chemical platform molecules.[4−9] The addition of a catalyst in the pyrolysis reactor has been shown to enhance control over the product distribution through selective conversion of the vapor phase products into valuable hydrocarbon products. Although many catalysts have been studied in fast pyrolysis,[5,10−12] perhaps the most widely studied catalyst is HZSM-5 because of its high selectivity to gasoline range hydrocarbons.[13−17] However, large quantities of water and coke are typically observed with its use.[18] Therefore, new catalysts are needed which can provide similar or improved catalytic activities and/or selectivities to other valuable products while generating less coke and therefore decreasing catalyst deactivation.[19−21]

In recent years, hierarchical zeolites, which contain both microporosity and mesoporosity, have been synthesized to exploit the shape selective properties of microporous zeolites while decreasing the diffusion and accessibility limitations of larger molecules in biomass upgrading.[22,23] In addition, the incorporation of mesopores in the zeolite material can reduce pore blocking caused by large molecules adsorbing to the surface, and it can thus decrease carbon deposition on and deactivation of the catalyst. For example, Resasco and co-workers reported coke reduction with a mesoporous HZSM-5 catalyst prepared by desilication in the conversion of propanal to gasoline range hydrocarbons.[24]

The incorporation of cerium into heterogeneous catalysts can also confer desirable properties. Cerium has been shown to reduce coke formation in recent work in gasification,[25−27] hexane isomerization,[28] and steam reforming[29−31] reactions. Elbaba et al. reported a Ni/CeO_2/alumina catalyst that decreased coke formation in waste tire gasification.[25] Cerium supported on zeolites showed a decrease in coke formation in

Received: December 9, 2011
Revised: March 13, 2012
Published: March 15, 2012

   dx.doi.org/10.1021/cs200648q | ACS Catal. 2012, 2, 642−646

Table 1. Physical and Chemical Properties of Studied Catalysts

material	wt % Ce[a]	Si/Al	S_{BET} (m^2/g)	V_{micro}[d] (cm^3/g)	S_{micro}[d] (m^2/g)	$S_{external}$[d] (m^2/g)	pore size (Å)[e]
HZSM-5-C	0	50[b]	392	0.167	329	63.4	
Meso-HZSM-5	0	49[c]	378	0.146	289	88.5	155
Meso-Ce-HZSM-5	1.92	55[c]	351	0.136	268	83.3	110
IW-Meso-HZSM-5	2.75	49[c]	198	0.070	134	64.0	111
Ex(3x)-HZSM-5-C	1.05	50[b]	279	0.118	230	49.1	

[a]ICP-OES. [b]From Vendor. [c]EDXS. [d]t-Plot Method. [e]BJH Desorption.

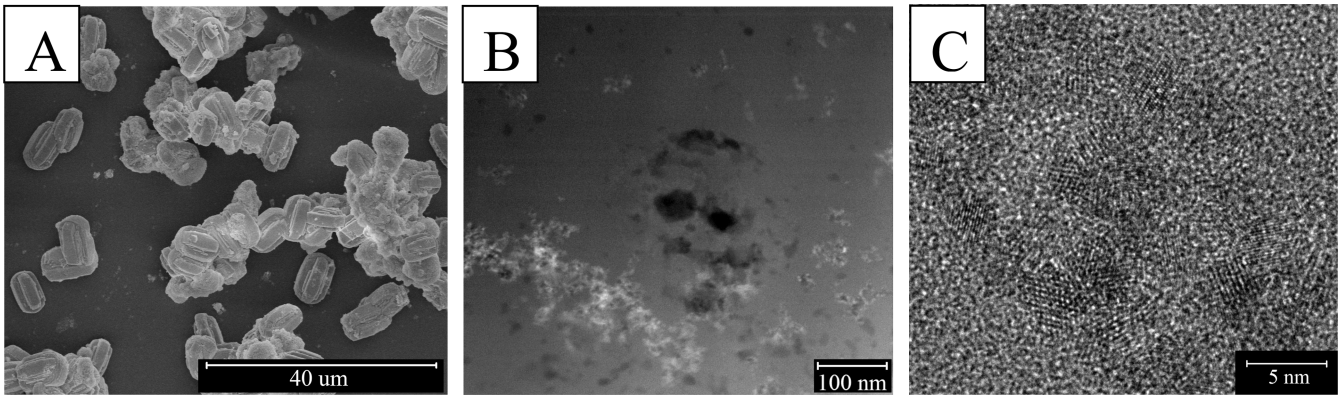

Figure 1. (A) SEM image of Meso-Ce-HZSM-5. (B) Dark field STEM image of Meso-Ce-HZSM-5. (C) TEM image of Meso-Ce-HZSM-5.

gasification of cellulose or polypropylene.[26,27] Cerium-based catalysts have also been used in catalytic fast pyrolysis. Bridgwater and co-workers reported an improvement in bio-oil properties from the catalytic fast pyrolysis of lignin-derived compounds with the use of MI-575 (a commercial cerium-based catalyst).[5] The addition of cerium to a Pd/TiO_2 catalyst for fast pyrolysis was found to aid in the conversion of lignin derived molecules into monomeric phenols.[12] In this contribution, we report the synthesis and performance of a novel HZSM-5 catalyst that was designed to incorporate both mesopores and cerium to optimize catalytic conversion and selectivity to value added compounds with high carbon efficiencies. This catalyst shows a reduction in coke formation relative to the commercial HZSM-5 catalyst for the catalytic fast pyrolysis of glucose and provides a pathway to alternate product selectivities to useful chemicals while maintaining activity.

RESULTS AND DISCUSSION

The cerium containing micro/mesoporous HZSM-5 material, Meso-Ce-ZSM-5, was synthesized by incorporating cerium nitrate into a dual templating method reported by Zhou et al.[22] Initially, a triblock copolymer (F127) was dissolved in DI water. Tetraethylorthosilicate (TEOS), aluminum isopropoxide, and cerium nitrate hexahydrate ($CeNO_3{\cdot}6H_2O$) were added to the template solution and stirred for 1 h at 40 °C. After one additional hour, tetrapropylammonium hydroxide (TPAOH) was added to the solution as the micropore structure-directing agent. The solution was stirred at 40 °C for 24 h, aged at 60 °C for 16 h, and dried at 90 °C overnight. The resulting solid was collected, steamed using a steam assisted crystallization step (SAC), and calcined to form the catalyst (Meso-Ce-ZSM-5). In this letter, Meso-Ce-HZSM-5, with cerium incorporated in the framework, with 1.92 wt % Ce and a Si/Al ratio of 55 is reported. This material was compared with four other materials to determine how cerium incorporation affects catalytic properties in the catalytic fast pyrolysis of glucose (Table 1): (1) commercial H-ZSM-5 (HZSM-5-C), (2) mesoporous H-ZSM5 (Meso-HZSM-5), (3) cerium added by incipient wetness (IW-Meso-ZSM-5), and (4) cerium added via ion-exchanged (Ex(3x)-HZSM-5-C).

X-ray diffraction (XRD) was performed on the new material before and after the steaming step. The steaming step was necessary to crystallize the catalysts synthesized by the dry gel method (Figure S9, Supporting Information).[22] The XRD patterns (Figures S2−S8, Supporting Information) show characteristic peaks for an MFI type zeolite at 2Θ angles of ∼8° and 23°.[32] The amount of cerium incorporated in Meso-Ce-HZSM-5 was determined by ICP-OES (Table 1). The amount of cerium added to the initial solution led to a theoretical incorporation of ∼2.25 wt % Ce, but the synthesized material had an actual loading of 1.92 wt % Ce. Thus, approximately 85% of the cerium added to the precursor solution was retained in the final material. Nitrogen physisorption was used to determine the pore diameter (Barret−Joyner−Halenda (BJH) method), surface areas (Brunauer−Emmett−Teller (BET) method), and pore volumes (t-plot method) of the catalysts. As shown in Table 1, Meso-Ce-HZSM-5 had mesopores with pore diameters of ∼110 Å. The micropore volume of this material was calculated to be ∼0.136 cc/g by the t-plot method which was similar to the noncerium containing mesoporous catalyst (Meso-HZSM-5) and which is typical for HZSM-5.[33]

SEM of Meso-Ce-HZSM-5 (Figure 1 A) shows particles possessing a twinned prism-like morphology with a nonsmooth surface and particle size of 9 μm. For scanning transmission electron microscopy (STEM) (Figure 1 B) and transmission electron microscopy (TEM) (Figure 1 C), the catalyst particle was prepared by cutting it into a thin sample using a focused ion beam (FIB). The STEM and TEM images show pockets of cerium incorporated within the catalyst particles. The dark field STEM image shows a white contrast for the cerium nanoparticles, whereas the dark spots correspond to mesopores within the sample. The TEM (Figure 1 C) was focused on a

dx.doi.org/10.1021/cs200648q | ACS Catal. 2012, 2, 642−646

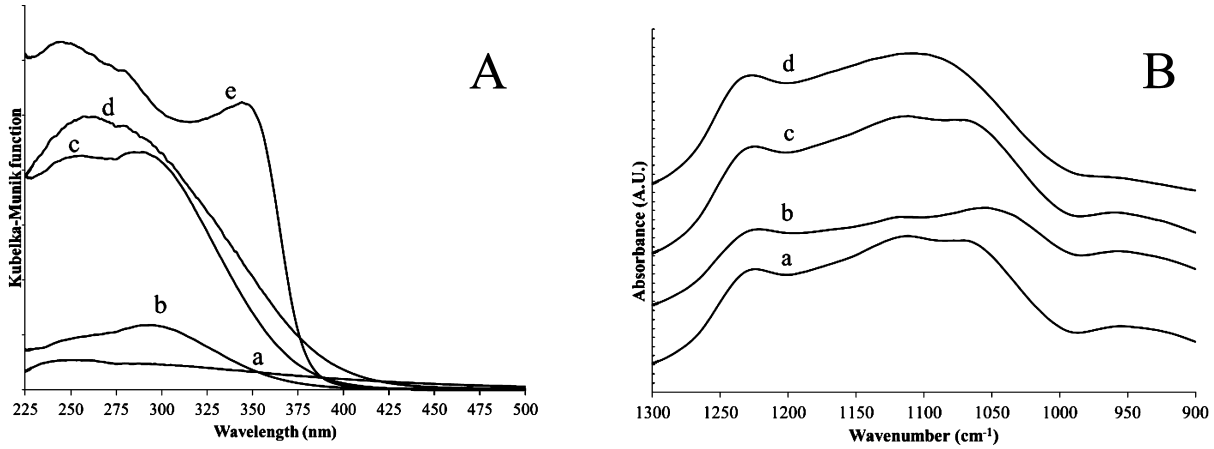

Figure 2. (A) Diffuse reflectance UV−Vis spectra of (a) Meso-HZSM-5, (b) Ex(3x)-HZSM-5-C, (c) IW-Meso-HZSM-5, (d) Meso-Ce-HZSM-5, (e) Bulk CeO_2. (B) IR spectra in the framework region of varying synthesis methods (a) Meso-HZSM-5, (b) Meso-Ce-HZSM-5, (c) IW-Meso-HZSM-5, (d) Ex(3x)-HZSM-5-C.

cluster of cerium within the sample. As shown in the image, the lattice fringes around the cerium cluster correspond to a face centered cubic (f.c.c.) fluorite structure in a CeO_{2-x} form (x = 0.16) with a lattice parameter of 5.48 Å. In comparison to CeO_2, with a lattice parameter of 5.41 Å, this increase is due to the presence of Ce^{3+} and O^{2-} vacancies in the structure.[34]

Diffuse reflectance UV−Vis was used to probe whether the incorporated cerium in the Meso-Ce-HZSM-5 was intra-framework or extra-framework. Bulk CeO_2 (Figure 2 A(e)) showed a large absorption band at ∼370 nm, which agrees with literature reports.[35] The Meso-HZSM-5 (Figure 2 A(a)) shows very low absorbance because of the absence of cerium. The Meso-Ce-HZSM-5 material shows a strong absorption at ∼260 nm, which is assigned to the charge transfer of O^{2-} to Ce^{3+}, indicating the incorporation of cerium into the framework.[35,36] The UV−Vis spectra of the cerium nitrate triple-exchanged commerical ZSM-5 (Ex(3x)-HZSM-5-C) with a cerium loading of 1.05 wt % and the incipient wetness (IW-Meso-HZSM-5) with a cerium loading of 2.75 wt % control materials (Figure 2 A (b) and (c), respectively) show peaks shifted toward lower energies, which correspond to extra-framework cerium bulk phases.[37] Although there is a strong peak at 260 nm in the Meso-Ce-HZSM-5, it is possible that both intra-framework and extra-framework cerium species are present because of the broadness of the large absorption band.

Diffuse reflectance FT-IR spectra (Figure 2 B) were obtained for Meso-HZSM-5, Meso-Ce-HZSM-5, IW-Meso-HZSM-5, and Ex(3x)-HZSM-5-C. Because the vibrations of Si−O and Si−O−Ce both appear at the same wavenumber, 970 cm^{-1}, this absorbance band cannot definitively indicate intra-framework cerium incorporation.[38] The absorbance band around 1070 cm^{-1} was assigned to the ν_{as}(Si−O−Si). A shift of 15 wavenumbers to 1055 cm^{-1} was noticed in the spectrum of Meso-Ce-HZSM-5 (Figure 2 B(b)), which is characteristic of the incorporation of cerium into the framework.[38,39] When cerium was added to the control catalysts (Figure 2 B(c) and (d)), this shift was not observed. Lastly, X-ray photoelectron spectroscopy (XPS) was used to probe the oxidation state of the surface cerium present on Meso-Ce-HZSM-5. The XPS results (Figure S10, Supporting Information) show two binding energies at 864 and 913 eV that correspond to the $3d_{5/2}$ and $3d_{3/2}$ respectively, and these are attributed to an oxidation state of Ce^{3+} on the surface of these catalysts.[40] In the presence of Ce^{4+} species, a peak at ∼920 eV is typically observed,[40] but this peak is absent in our material, which suggests that Ce^{3+} is the primary species on the surface of the catalyst.

In the present work, the catalytic fast pyrolysis of glucose (a carbohydrate model compound) was studied at 600 °C in a Pyroprobe 5200 reactor. All of the catalysts (Table 1) were studied in this reactor with a feed to catalyst ratio of 1:9, a 1000 °C/s ramp rate, and 360 s residence time. The primary products from the pyrolysis of glucose with HZSM-5-C were benzene, toluene, xylenes, and naphthalenes (Figure 3 and Table 2). Using Ex(3x)-HZSM-5, the aromatic carbon selectivites were unaffected. The Meso-HZSM-5 catalyst (no cerium) also produced aromatics, but the selectivities to oxygenated chemicals increased. From NH_3-TPD (Figure S14, Supporting Information), the commercial HZSM-5 catalyst contained more acid sites compared to the Meso-HZSM-5 catalyst. We hypothesize that the reduction in the acidity of the mesoporous zeolite leads to increased yield of oxygenated chemicals. The IW-Meso-HZSM-5 catalyst also produced equivalent amounts of aromatics and oxygenated chemicals, with no noticeable effect due to cerium versus just

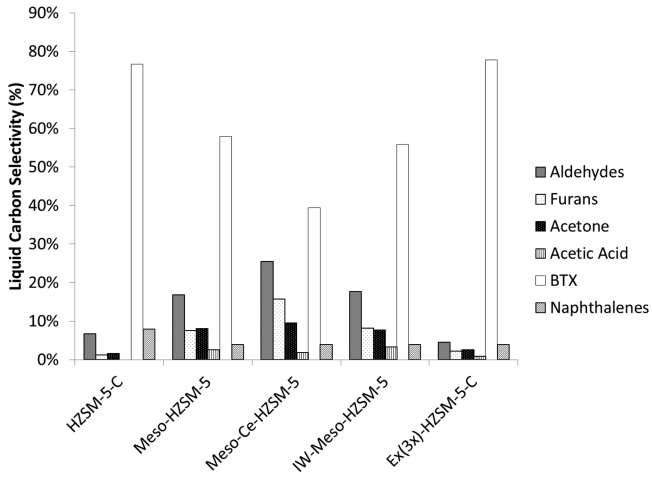

Figure 3. Molar carbon selectivity of catalytic fast pyrolysis of glucose comparing various catalysts. Key Aldehydes: acetaldehyde, furfural. Furans: furan, methyl-furan. BTX: benzene, toluene, xylenes. Naphthalenes: naphthalene, methyl-naphthalene.

dx.doi.org/10.1021/cs200648q | ACS Catal. 2012, 2, 642−646

Table 2. Summary of the Molar Carbon Yields and Liquid Selectivity of Catalytic Fast Pyrolysis of Glucose with Various Catalysts

catalyst	HZSM-5-C	Meso-HZSM-5	Meso-Ce-HZSM-5	IW-Meso-HZSM-5	Ex(3x)-HZSM-5-C
			Overall Carbon Yield (%)		
aromatics	24.1	21.3	11.3	13.0	28.8
oxygenates	2.4	11.5	12.3	7.4	3.3
CO	18.7	16.0	21.8	22.4	18.6
CO_2	9.6	3.8	5.1	5.9	4.9
light gases	2.9	3.0	3.6	3.8	1.2
coke	43.8	42.0	39.2	45.4	42.9
total	101.6	97.6	93.2	98.0	99.7
			Liquid Carbon Selectivity (%)		
acetaldehyde	6.7	16.6	25.0	17.3	4.4
furfural	0.0	0.2	0.4	0.3	0.0
furan	1.2	6.2	12.5	6.4	1.8
methyl furan	0.0	1.3	3.2	1.7	0.3
acetone	1.5	8.1	9.5	7.6	2.5
acetic acid	0.0	2.6	1.8	3.2	0.8
benzene	12.5	7.1	6.9	8.5	13.5
toluene	48.5	40.4	17.3	32.8	52.2
xylenes	15.7	10.4	15.2	14.6	12.1
naphthalenes	13.9	7.2	8.2	7.6	12.3

[a]Reactions were run at 600 °C with a heating rate of 1000 °C/s and a reaction time of 360 s.

the incorporation of mesoporosity. However, the Meso-Ce-HZSM-5 catalyst showed a remarkable shift in selectivities to more oxygenated chemicals than aromatics (Figure 3 and Table 2), much greater than what was observed with mesopore incorporation alone. Furthermore, the overall acidity of Meso-Ce-HZSM-5 decreased. The intra-framework Ce catalyst (Meso-Ce-HZSM-5) produced more acetone than all the other tested catalysts and less acetic acid than the other mesoporous catalysts. Since the ketonization of carboxylic acids has been well studied as a method to stabilize pyrolysis oils,[41,42] we investigated this catalyst's ability to upgrade acetic acid to acetone under reaction conditions. It was found that Meso-Ce-HZSM-5 was able to ketonize acetic acid to form acetone (Scheme 1 and Table S2, Supporting Information) in much

Scheme 1. Ketonization of Acetic Acid with Mesoporous Catalysts

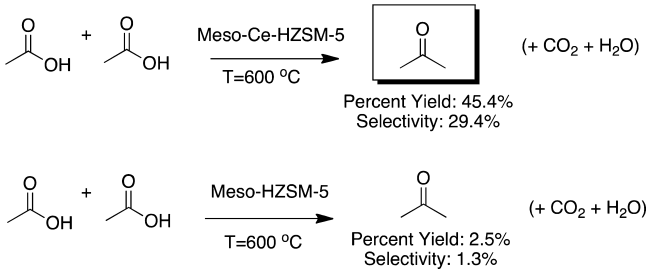

higher percent yields (45.4%) than noncerium containing Meso-HZSM-5 (2.5%), Ex(3x)-HZSM-5 (4.4%), and IW-Meso-HZSM-5 (6.4%).[43] These results indicate that Meso-Ce-HZSM-5 may also be able to improve bio-oils by upgrading formed carboxylic acids to more stable products.

With conventional HZSM-5 catalysts, large coke production is commonly observed, which suggests the need for catalysts with higher carbon efficiencies. Hierarchical zeolites are believed to improve performance over conventional HZSM-5 by decreasing diffusion limitations, allowing larger molecules to both enter and escape the porous network more easily, thus improving a catalyst's resistance to coking. Cerium is also believed to play a role in coke reduction as outlined in the introduction. Coke formation decreased significantly from 34 wt % using commercial HZSM-5 (HZSM-5-C) to 20 wt % with Meso-Ce-HZSM-5 (Figure S16, Supporting Information) and decreased 11% by molar carbon yield (Table 2). Along with catalyst coke reduction, an increase in decarbonylation reactions to form CO was observed with the Meso-Ce-HZSM-5 catalyst.

The regeneration and recyclability of these catalysts was also studied. A drastic reduction in micropore volume after the first use indicates that the coke that is formed is primarily located on the micropore surfaces. The used Meso-Ce-HZSM-5 was regenerated at 630 °C for 30 min after a ramp of 2 °C/min. The N_2 physisoprtion data (Table S1, Supporting Information) shows the removal of carbon deposits and the persistence of mesopores. After regenerating the catalyst, low catalyst coke formation during reaction was maintained (Figure S15, Supporting Information). After the catalyst was regenerated, the catalyst showed a high selectivity to chemicals production from glucose.

CONCLUSION

The synthesis of cerium-incorporated hierarchical HZSM-5 catalysts with the benefits of high selectivities to chemicals from biomass and low catalyst coking was achieved. Experimental evidence suggests the presence of cerium incorporation in the framework and reduced acidity are responsible for the marked shift in selectivities and decrease in coke formation compared to commercial HZSM-5. Furthermore, the cerium-incorporated catalyst was capable of performing ketonization of carboxylic acids and thus stabilizing the resulting pyrolysis oil. These multifunctional catalysts maintained selectivities and activities upon regeneration and recycling.

dx.doi.org/10.1021/cs200648q | ACS Catal. 2012, 2, 642–646

■ ASSOCIATED CONTENT

Supporting Information

Materials synthesis, characterization, experimental conditions, and calculations. This material is available free of charge via the Internet at http://pubs.acs.org.

■ AUTHOR INFORMATION

Corresponding Author

*E-mail: jhicks3@nd.edu.

Notes

The authors declare no competing financial interest.

■ ACKNOWLEDGMENTS

We thank the Center for Environmental Science and Technology at University of Notre Dame for the use of the center's Bruker FTIR and Perkin-Elmer ICP-OES. We also thank Tatyana Orlova for preparing samples in the focused ion beam and Dr. Thomas Kosel for assisting with STEM and TEM.

■ REFERENCES

(1) Choi, S.; Drese, J. H.; Jones, C. W. *ChemSusChem* **2009**, *2*, 796–854.

(2) Huber, G. W.; Iborra, S.; Corma, A. *Chem. Rev.* **2006**, *106*, 4044–4098.

(3) Zakzeski, J.; Bruijnincx, P. C. A.; Jongerius, A. L.; Weckhuysen, B. M. *Chem. Rev.* **2010**, *110*, 3552–3599.

(4) Aho, A.; Kumar, N.; Eränen, K.; Salmi, T.; Hupa, M.; Murzin, D. Y. *Fuel* **2008**, *87*, 2493–2501.

(5) Pattiya, A.; Titiloye, J. O.; Bridgwater, A. V. *J. Anal. Appl. Pyrol.* **2008**, *81*, 72–79.

(6) Corma, A.; Huber, G. W.; Sauvanaud, L.; O'Connor, P. *J. Catal.* **2007**, *247*, 307–327.

(7) French, R.; Czernik, S. *Fuel. Process. Technol.* **2010**, *91*, 25–32.

(8) Olazar, M.; Aguado, R.; Bilbao, J.; Barona, A. *AIChE J.* **2000**, *46*, 1025–1033.

(9) Williams, P. T.; Horne, P. A. *J. Anal. Appl. Pyrol.* **1995**, *31*, 39–61.

(10) Lu, Q.; Xiong, W. M.; Li, W. Z.; Guo, Q. X.; Zhu, X. F. *Bioresour. Technol.* **2009**, *100*, 4871–4876.

(11) Fahmi, R.; Bridgwater, A. V.; Darvell, L. I.; Jones, J. M.; Yates, N.; Thain, S.; Donnison, I. S. *Fuel* **2007**, *86*, 1560–1569.

(12) Lu, Q.; Zhang, Y.; Tang, Z.; Li, W. Z.; Zhu, X. F. *Fuel* **2010**, *89*, 2096–2103.

(13) Carlson, T. R.; Cheng, Y. T.; Jae, J.; Huber, G. W. *Energy Environ. Sci.* **2011**, *4*, 145–161.

(14) Carlson, T. R.; Tompsett, G. A.; Conner, W. C.; Huber, G. W. *Top. Catal.* **2009**, *52*, 241–252.

(15) Chen, N. Y.; Degnan, T. F.; Koenig, L. R. *CHEMTECH* **1986**, *16*, 506–511.

(16) Jae, J.; Tompsett, G. A.; Foster, A. J.; Hammond, K. D.; Auerbach, S. M.; Lobo, R. F.; Huber, G. W. *J. Catal.* **2011**, *279*, 257–268.

(17) Zhang, H. Y.; Cheng, Y. T.; Vispute, T. P.; Xiao, R.; Huber, G. W. *Energy Environ. Sci.* **2011**, *4*, 2297–2307.

(18) Lappas, A. A.; Samolada, M. C.; Iatridis, D. K.; Voutetakis, S. S.; Vasalos, I. A. *Fuel* **2002**, *81*, 2087–2095.

(19) Hicks, J. C. *J. Phys. Chem. Lett.* **2011**, *2*, 2280–2287.

(20) Lin, Y. C.; Huber, G. W. *Energy Environ. Sci.* **2009**, *2*, 68–80.

(21) Rinaldi, R.; Schüth, F. *Energy Environ. Sci.* **2009**, *2*, 610–626.

(22) Zhou, J.; Hua, Z.; Liu, Z.; Wu, W.; Zhu, Y.; Shi, J. *ACS Catal.* **2011**, *1*, 287–291.

(23) Chal, R.; Gerardin, C.; Bulut, M.; van Donk, S. *ChemCatChem* **2011**, *3*, 67–81.

(24) Zhu, X. L.; Lobban, L. L.; Mallinson, R. G.; Resasco, D. E. *J. Catal.* **2010**, *271*, 88–98.

(25) Elbaba, I. F.; Wu, C.; Williams, P. T. *Int. J. Hydrogen Energy* **2011**, *36*, 6628–6637.

(26) Inaba, M.; Murata, K.; Saito, M.; Takahara, I. *Energy Fuels* **2006**, *20*, 432–438.

(27) Wu, C. F.; Williams, P. T. *Int. J. Hydrogen Energy* **2009**, *34*, 6242–6252.

(28) Jongpatiwut, S.; Sackamduang, P.; Rirksomboon, T.; Osuwan, S.; Alvarez, W. E.; Resasco, D. E. *Appl. Catal., A* **2002**, *230*, 177–193.

(29) Stagg-Williams, S. M.; Noronha, F. B.; Fendley, G.; Resasco, D. E. *J. Catal.* **2000**, *194*, 240–249.

(30) Ma, L.; Praharso; Trimm, D. L. *Rare Earths '98* **1999**, *315–3*, 187–193.

(31) Laosiripojana, N.; Sangtongkitcharoen, W.; Assabumrungrat, S. *Fuel* **2006**, *85*, 323–332.

(32) Wu, E. L.; Lawton, S. L.; Olson, D. H.; Rohrman, A. C.; Kokotailo, G. T. *J. Phys. Chem.* **1979**, *83*, 2777–2781.

(33) Voogd, P.; Scholten, J. J. F.; van Bekkum, H. *Colloids Surf.* **1991**, *55*, 163–171.

(34) Trovarelli, A. *Catalysis by ceria and related materials*; Imperial College Press: London, U.K., 2002; Vol. *2*, p 527.

(35) Yuliati, L.; Hamajima, T.; Hattori, T.; Yoshida, H. *Chem. Commun.* **2005**, 4824–4826.

(36) Strunk, J.; Vining, W. C.; Bell, A. T. *J. Phys. Chem. C* **2011**, *115*, 4114–4126.

(37) Devika, S.; Palanichamy, M.; Murugesan, V. *J. Mol. Catal. A: Chem.* **2011**, *351*, 136–142.

(38) Laha, S. C.; Mukherjee, P.; Sainkar, S. R.; Kumar, R. *J. Catal.* **2002**, *207*, 213–223.

(39) As reported by Laha et al.[38] for Ce-MCM-41 materials, an absorbance band around 1090 cm^{-1} was observed for this ν_{as}(Si-O-Si) transition. With Al also present in the framework of the Meso-HZSM-5 materials, a shift to lower wavenumbers is observed (~1070 cm^{-1} for Si:Al 50). The large shift of 15 wavenumbers in Meso-Ce-HZSM-5 is primarily due to the presence of Ce in the framework, since the Si:Al ratio of this material was higher than 50.

(40) Zhang, F.; Wang, P.; Koberstein, J.; Khalid, S.; Chan, S. W. *Surf. Sci.* **2004**, *563*, 74–82.

(41) Gartner, C. A.; Serrano-Ruiz, J. C.; Braden, D. J.; Dumesic, J. A. *ChemSusChem* **2009**, *2*, 1121–1124.

(42) Vivier, L.; Duprez, D. *ChemSusChem* **2010**, *3*, 654–678.

(43) Percent Yield was calcuated by dividing the moles of acetone produced by the maximum moles of acetone possible (theoretical) × 100%. The selectivities were calculated by dividing the moles of acetone produced by the moles of other products produced and multiplying by 100%.